IMPROVEMENT IN CREEP STRENGTH OF ADVANCED HEAT RESISTANT STEEL BASED FERRITE MATRIX

Yoshiaki Toda, Hideaki Kushima, Kazuhiro Kimura and Fujio Abe
National Institute for Materials Science, Japan

ABSTRACT

The effects of nickel content and heat treatment conditions on the creep strength of precipitation-strengthened 15Cr ferritic steel were investigated. The creep strength of the 15Cr ferritic steel was drastically improved by solution treatment and water quenching. However, over the long term, the detrimental effect of nickel on the creep strength was pronounced for water-quenched steels. The volume fraction of martensite phase increased with increased nickel content in both the furnace-cooled and water-quenched steels. The volume fraction of martensite phase in the water-quenched steel was smaller than that in the furnace-cooled type, even for the same nickel content. Fine particles, smaller than 500 nm, were precipitated homogeneously within the ferrite phase of the water-quenched steel. On the other hand, coarse block-like particles 1 μm in size were precipitated sparsely within the martensite phase, and the recovery of martensitic microstructure was accelerated. The creep strength of the steels decreased with increased volume fraction of the martensite phase caused by furnace cooling and nickel addition. The lower creep strength and microstructural stability of the martensite phase is attributable to less precipitation strengthening. To enable this steel to be put to practical use, it will be necessary to suppress the formation of the martensite phase caused by addition of nickel by optimizing the chemical composition and heat treatment conditions.

KEY WORDS

Creep; Ferrite matrix; Furnace cooling; Intermetallic compound; Martensite phase; Nickel content; Recovery; Water quenching

1. INTRODUCTION

To save fossil fuel resources and reduce CO_2 emissions, considerable efforts have been directed towards the research and development of high-strength, creep-resistant steels and alloys to improve the energy efficiency of power plants [1]. Since the energy efficiency of fossil fuel-burning power plants can be improved by increasing their steam temperature and pressure, high-strength, heat-resistant materials need to be developed. Ferritic heat-resistant steel is suitable for large and thick structural components that are exposed to high temperatures, such as headers and main steam pipes, so it is in wide use in power plants. The microstructure of conventional ferritic heat-resistant steel is usually tempered martensite strengthened by numerous precipitates of carbide and MX-type carbonitride. However, microstructural degradation due to preferential recovery at the vicinity of prior austenite grain boundaries results in decreased creep strength, especially in the long term [2-4]. Both creep strength and oxidation resistance need to be improved in high-temperature structural materials to enable them to withstand higher steam temperatures and pressures. Although chromium is the most effective alloying element for improving oxidation resistance, maximum chromium concentration is restricted to about 11 mass% and below in conventional high strength ferritic heat-resistant steel to avoid the formation of δ-ferrite, a phase that is detrimental to creep strength and fracture toughness. Improvements in both long-term creep strength and oxidation resistance are important for the development of high strength ferritic heat-resistant steel.

HOME

The improvement in long-term creep strength of a 15Cr ferritic steel with an annealed ferrite matrix instead of a tempered martensitic microstructure in conventional ferritic heat-resistant steels has been investigated from the above perspectives [5-11]. Kimura et al. reported that the creep strength of 15Cr ferritic steel could be improved by additions of tungsten and cobalt through precipitation-strengthening effects of intermetallic compounds [5-8]. Toda et al. found that concentrations of carbon and nitrogen strongly affect the stability of microstructures in precipitation-strengthened 15Cr ferritic steel [9]. It has been discovered that higher long-term creep strength in the 15Cr steel than that of conventional steels could be obtained by optimizing carbon and nitrogen content through small coarsening rates of fine particles and homogeneous distribution of those without precipitation-free zones [9]. Moreover, it was found that the addition of nickel and an increase in cooling rate from the annealing temperature improved the impact toughness of precipitation-strengthened 15Cr ferritic steel, although it has been pointed out that 15Cr steel has the drawback of poor toughness due to the presence of ferrite matrix [10, 11]. However, the effects of nickel content and rapid cooling on creep strength of the 15Cr steel have not yet been sufficiently elucidated. The aim of the present study is, therefore, to investigate the effects of nickel content and heat treatment conditions on the creep strength of a precipitation-strengthened 15Cr ferritic steel.

2. EXPERIMENTAL PROCEDURE

The chemical compositions of the steels used in the present study are shown in Table 1. The base material was nickel-free 0.05C-15Cr-1Mo-0.2V-0.05Nb-6W-3Co-0.04N-0.003B (mass%) steel, which possessed superior creep strength [9]. The other five steels used contained 0.4, 0.8, 1.2, 1.6 and 2.0 mass% nickel. These steels were prepared in a vacuum induction furnace. Ingots with a weight of 10 kg were hot forged into bars 15 mm in diameter and solution-treated for 30 min at 1473 K followed by furnace cooling. Water-quenched steels were also used to investigate the effects of heat treatment on the creep strength.

The dimensions of the creep test specimen were 6 mm in gauge diameter and 30 mm in gauge length according to Type 14A of the Japanese Industrial Standard (JIS) Z 2201 [12]. Creep tests were conducted at 923 K and over a range of stresses from 100 MPa to 240 MPa up to about 25000 h in air. Creep deformation was measured using an extensometer attached to the gauge portion of the specimen. The microstructure of the specimens was examined under an optical microscope (OM), a scanning electron microscope (SEM), and a transmission electron microscope (TEM). Concentrations and structures in the matrix and precipitates were measured using energy-dispersive X-ray fluorescence spectrometry (EDX) and X-ray analysis. “Thermo-Calc” thermodynamic calculation software was used to predict the mole fractions of equilibrium phases in the steels.

Table 1 Chemical compositions of the steels used in the present study (mass%).

	C	Ni	Cr	Mo	W	V	Nb	Co	N	B
Base	0.046	<0.01	15.00	1.00	6.07	0.19	0.043	2.97	0.033	0.0030
0.4Ni	0.047	0.42	14.93	1.00	6.05	0.20	0.050	2.96	0.041	0.0029
0.8Ni	0.048	0.78	15.00	1.00	6.05	0.20	0.050	2.96	0.042	0.0029
1.2Ni	0.049	1.21	15.02	1.00	6.04	0.20	0.051	2.96	0.042	0.0028
1.6Ni	0.048	1.60	15.00	1.00	6.03	0.20	0.050	2.95	0.044	0.0026
2.0Ni	0.048	2.00	14.96	0.99	6.07	0.20	0.050	2.98	0.036	0.0029

HOME

3. RESULTS

3.1. Creep strength

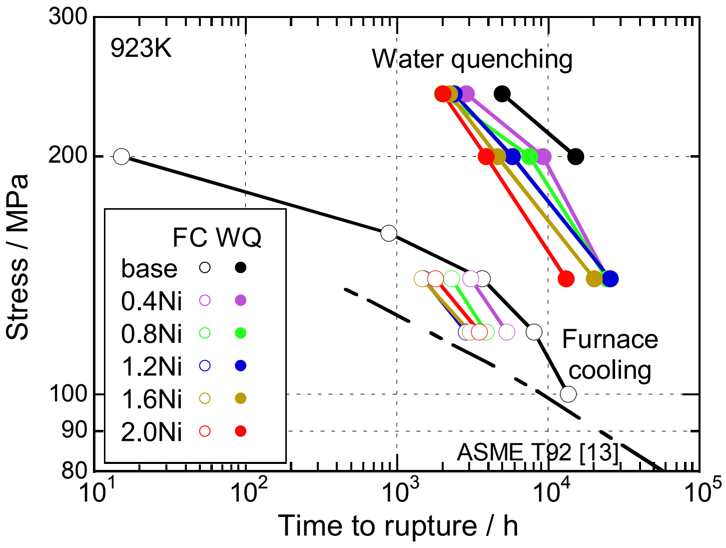

Fig. 1. Stress vs. time to rupture curves of the furnace-cooled and the water-quenched steels with the various nickel contents and the conventional heat resistant steel[13)] at 923K.

Figure 1 shows stress vs. time-to-rupture curves at 923 K of the furnace-cooled and the water-quenched steels with various nickel contents. The curve for 9Cr-0.5Mo-1.8W-V-Nb steel (ASME T92), which is conventional ferritic heat-resistant steel with a tempered martensitic microstructure, and which possesses the highest creep strength of the conventional steels [13], is also shown by the dashed curve in the same Figure. Regardless of nickel content, the creep strength of the furnace-cooled steels was slightly higher than that of ASME T92 [13]. Moreover, the creep strength of the 15Cr steel was drastically improved by solution treatment and water quenching regardless of Ni content; notably, the creep rupture life of the water-quenched 0.4Ni steel was 9203.6 h at 200 MPa. The creep strength at 10^4 h of this steel was double that of the conventional version, and the creep rupture life at 200 MPa was extended by a factor of approximately 1000. However, time to rupture of the water-quenched steels tended to decrease with increased nickel concentration, and the slope of the curves increased under low stress over the long term.

Figure 2 shows creep rate vs. time curves of the furnace-cooled base steel and the water-quenched steels with various nickel contents at 140 MPa and 923 K. The water-quenched base steel had not yet ruptured after 16000 h under these stress conditions. The creep rates of the water-quenched steels were about one tenth that of the furnace-cooled version just after loading, and continued to decrease during the transient creep stage. The creep rupture lives of the water-quenched steels extended to longer than those of the furnace-cooled versions. However, among the water-quenched steels, the onset time of the accelerating creep stage and creep rupture lives tend to shorten with increased nickel content.

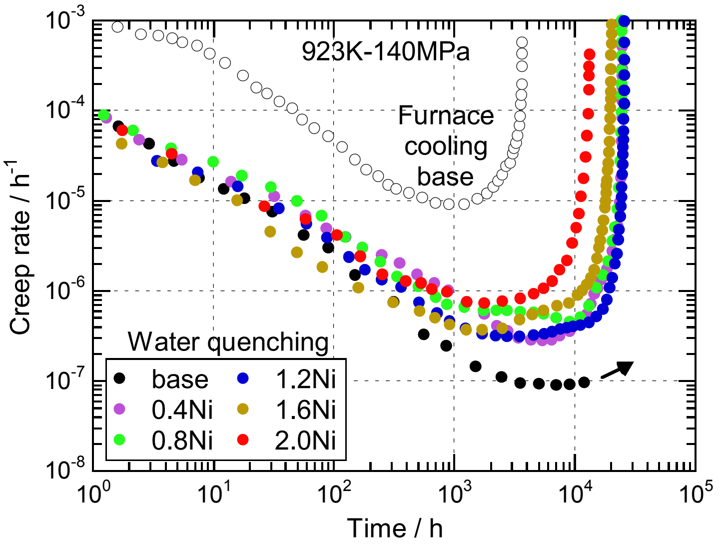

Fig. 2. Creep rate vs. time curves of the furnace-cooled base steel and the water-quenched steels with the various nickel contents at 140MPa and 923K.

Figure 3 shows rupture elongation and reduction of area of the water-quenched steels ruptured at 923 K and the various stress conditions as a function of time to rupture. It was found that the addition of nickel

HOME

improved the elongation and slightly improved the reduction of area.

Creep strength of the precipitation-strengthened 15Cr ferritic steel was drastically increased by the solution treatment and water quenching, and nickel addition improved rupture elongation and slightly improved the reduction of area of the steel. However, nickel content was found to be detrimental to the creep strength of the water-quenched steel over the long term.

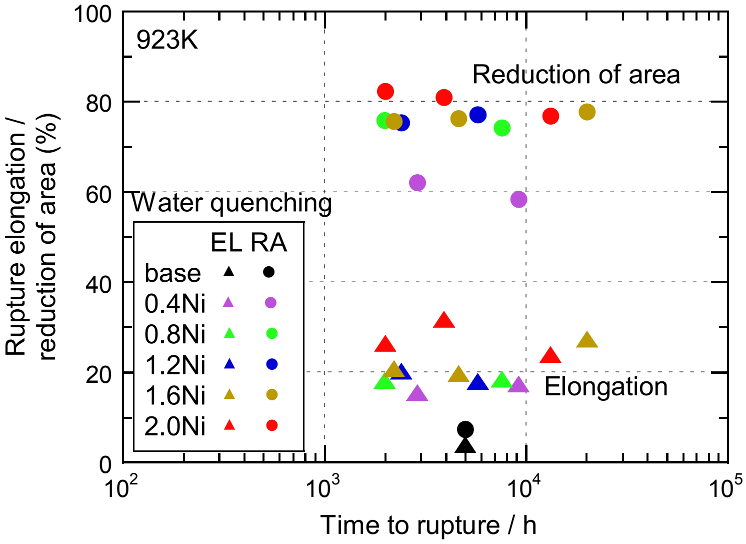

Fig. 3. Rupture elongation and reduction of area of the water-quenched steels creep-ruptured at 923K and the various stress conditions as a function of time to rupture.

3.2. Microstructure

3.2.1. Effect of heat treatment

Figure 4 shows OM images of (a) 0.0Ni; (b) 1.2Ni; (c) 2.0Ni steels after furnace cooling, and (d) 0.0Ni; (e) 1.2Ni; (f) 2.0Ni steels after water quenching. V_f marked on each photo indicates the volume fraction of the martensite phase. After furnace-cooling, a dense distribution of precipitates along the grain boundaries and coarse particles within the grains was observed in the base steel (Fig. 4 (a)). Some coarse block-type precipitates were formed on the grain boundaries of Ni-added steels (Fig. 4 (b), (c)). These precipitates in the furnace-cooled steels appear to have been formed during furnace cooling. On the other hand, precipitates were not clearly observed in the water-quenched steels, regardless of nickel content (Fig. 4 (d)–(f)). Rapid cooling appears to suppress the formation of coarse precipitates in the water-quenched steels.

X-ray diffraction analysis and concentration measurement by EDX were conducted to identify the

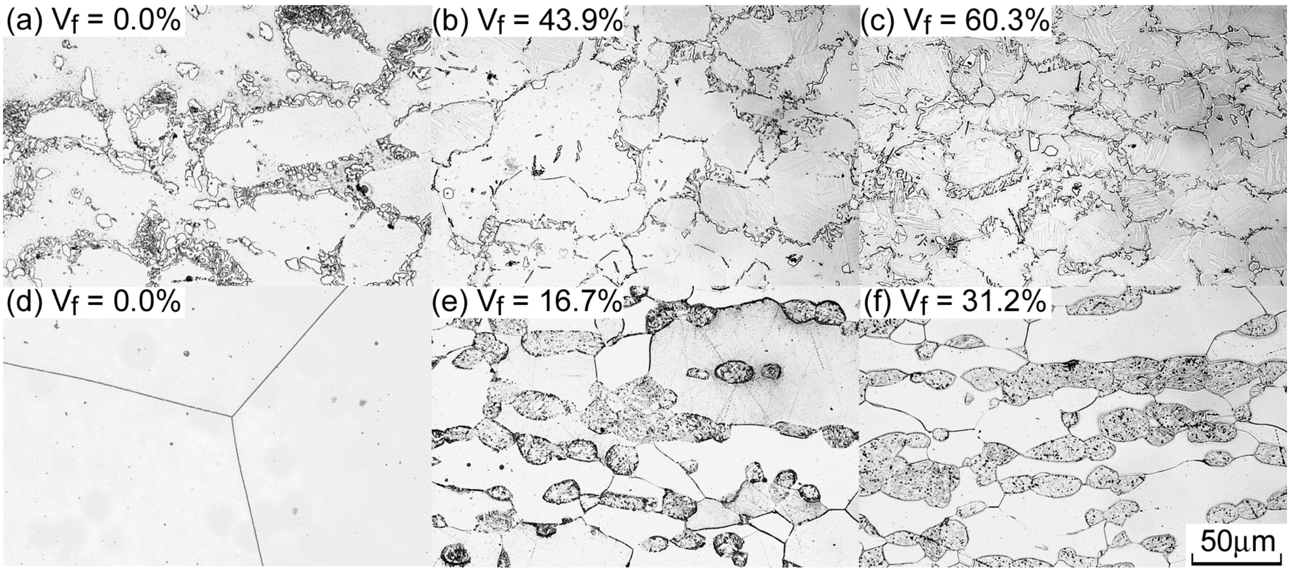

Fig. 4. OM images of (a) base; (b) 1.2%Ni; (c) 2.0%Ni steels in the as furnace-cooled condition and (d) base; (e) 1.2%Ni; (f) 2.0%Ni steels in the as water-quenched condition. V_f inserted into each photo stand for the volume fractions of martensite phase.

HOME

precipitates in the furnace-cooled base steel aged isothermally for 1000 h and 923 K. By comparing the obtained profiles with the Joint Committee on Powder Diffraction Standards cards, the peaks were identified as those from the χ-phase ($Fe_{36}Cr_{12}W_{10}$), the μ-phase (Fe_7W_6), the Laves phase (Fe_2W), which are intermetallic compounds classified into a topologically close-packed (TCP) phase [14], and a carbide ($M_{23}C_6$). And it was obvious that the concentrations of some precipitates, which were measured by EDX with TEM, chiefly comprised iron, chromium, molybdenum and tungsten. Therefore, the precipitates were identified by X-ray analysis and concentration measurement as the χ-phase or Laves phase, in which where chromium is in solid solution. The same intermetallic compounds appeared to be present in the furnace-cooled and nickel-added steels. Although the martensite phase was not observed in the furnace-cooled base steel (Fig. 4 (a)), it was observed within some grains with contrasts of block or packet boundaries in nickel-containing steels, and the volume fraction of martensite phase increased with increased nickel content (Fig. 4 (b), (c)). No martensite phase was detected in the water-quenched base steel (Fig. 4 (d)). However, many martensite phase grains 20–30 μm in diameter were observed along the grain boundaries of coarse ferrite grains with dark contrast in both the water-quenched and nickel-containing steels (Fig. 4 (e), (f)). As with the furnace-cooled steels, an increase in the volume fraction of the martensite phase was observed with increased nickel content in the water-quenched steels. The martensite phase was clearly observable in the water-quenched steels by its dark contrast; however, unlike in the furnace-cooled steels, the volume fraction of martensite phase in the furnace-cooled steels was about double that in the water-quenched version, even for the same nickel concentration.

It is thought generally that martensitic transformation requires a high cooling rate. The reason for the volume fraction of the martensite phase in the furnace-cooled steels being higher than that in the water-quenched steels can be assumed from temperature-dependence of the equilibrium fraction of the austenite phase. The solid curves in Figure 5 show calculated mole fractions of the austenite phase in these steels with the various nickel concentrations over a range of temperatures between 800 K and 1600 K. The open circles in the same Figure show the experimental volume fraction of martensite phase after water quenching from the solution-treated temperature of 1473 K. The mole fractions of the austenite phase at 1473 K were calculated to be about 5% in 1.2%Ni steel and 18% in 2.0%Ni steel, and were found to correspond to the experimental volume fractions of the martensite phase under water-quenched conditions. Moreover, it was indicated by calculation that the maximum mole fraction of the austenite phase was formed at the range of temperatures from 1173 K for 2.0%Ni steel to 1313 K for base steel. Therefore, the volume fraction of austenite phase increased during furnace cooling from the annealing temperature of 1473 K, and was followed by martensitic transformation at low temperature. On the other hand, the specimens were cooled quickly before the forming of the austenite phase in the water-quenched steels, which resulted in a higher volume fraction of martensite phase being seen in the

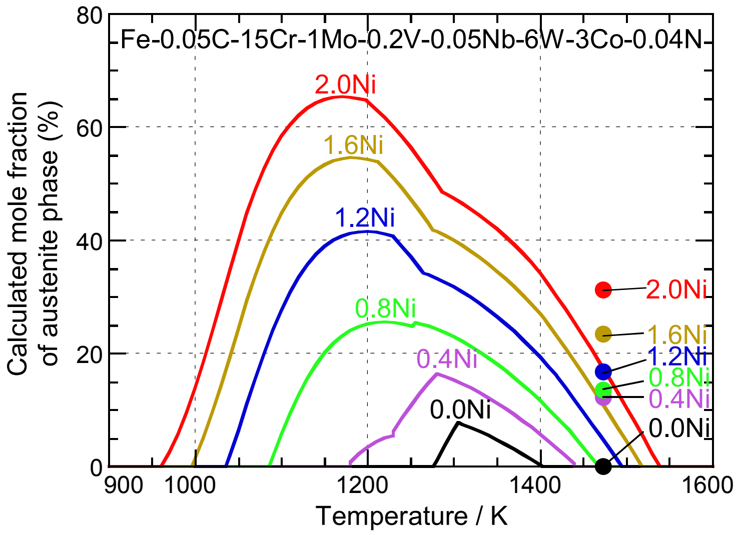

Fig. 5. The solid curves show changes in the calculated equilibrium mole fractions of austenite phase of the steels containing the various nickel contents with temperature. Open circles show the experimental volume fractions of martensite phase after water quenching.

HOME

furnace-cooled steels than in the water-quenched versions.

3.2.2. Effect of Ni content on water-quenched steels

Figure 6 shows SEM images of the water-quenched (a) 0.4%Ni; (b) 1.2%Ni and (c) 2.0%Ni steels creep-ruptured at 923 K and 200 MPa. t_r marked on each image indicates times to rupture. The grains 20–30 μm in size observed in the bottom half of each photo of Fig. 6 (b) 1.2%Ni steel and (c) 2.0%Ni steel are martensite phase that appears to have been transformed from the austenite phase at 1473 K or during water quenching. All of the matrix except for the martensite phase is the ferrite phase. Many particles smaller than 500 nm, which the results for isothermally aged steel suggest to have been precipitated during creep exposure, were observed homogeneously within the ferrite matrix in all the steels and remained small, even after several thousand hours of creep exposure. On the other hand, coarsened block-like particles 1 μm in size were precipitated sparsely within the martensite phase. With increased nickel content, the volume fraction of martensite phase increased, and the microstructure of the steels became markedly heterogeneous.

Table 2 shows the average compositions of the ferrite and the martensite phase in the 2.0%Ni steel after water-quenching measured by EDX. Elements accounting for less than 1 mass% were not measured. As a result, the concentration of nickel, which is an austenite former element, was higher in the martensite phase, and concentrations of tungsten and molybdenum, which are ferrite former elements, were lower than those in the ferrite phase. It is assumed that these elements were distributed to each phase at the solution treatment temperature of 1473 K.

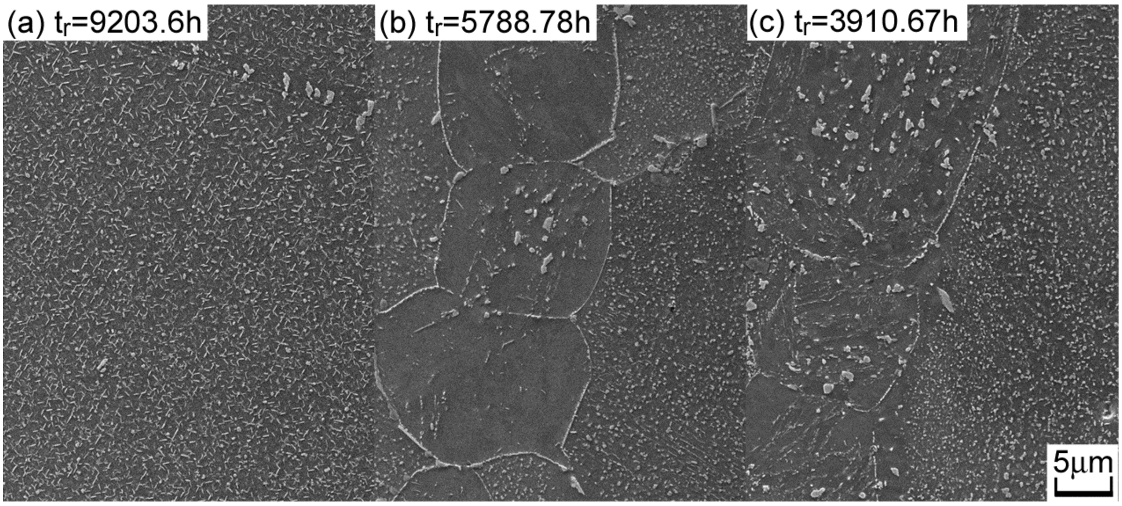

Fig. 6. SEM images of the water-quenched (a) 0.4%Ni; (b) 1.2%Ni; (c) 2.0%Ni steels creep-ruptured at 923K and 200MPa. t_r inserted into each photo stand for the time to rupture.

The precipitates of the 15Cr ferritic steel shown in Fig. 6 have been identified as topologically

Table 2 Average compositions of the martensite and the ferrite phase of 2.0%Ni steel in the as water-quenched condition (mass%).

	Fe	Ni	Cr	Mo	W	Co
Martensite phase	71.5	3.7	13.8	0.9	6.9	3.2
Ferrite phase	66.3	1.6	14.5	1.7	13.3	2.6

close-packed (TCP) phases, such as the Laves phase, χ phase and μ phase [5-9]. Figure 7 shows changes at 923 K in the calculated equilibrium mole fractions of TCP phases with nickel concentration of the steels containing different tungsten content. The equilibrium mole fractions of TCP phases decreased in proportion as nickel concentration increased to 1.2 mass%. It was no surprise that the mole fractions of these phases were small in steels with a low tungsten content. Therefore, since the driving force available for precipitation of TCP phases decreased through the high content of nickel and the low content of tungsten by element distribution at the solution treatment temperature, the coarsened precipitates were formed heterogeneously in the martensite phase.

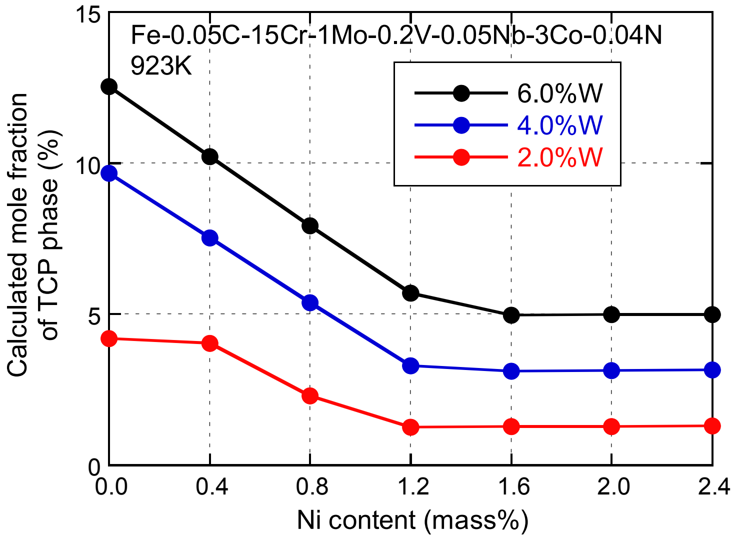

Fig. 7. Changes in the calculated equilibrium mole fractions of TCP phases with nickel concentration of the steels containing various tungsten contents at 923K.

Figure 8 shows a TEM image of 0.4%Ni steel creep-ruptured at 923 K and 200 MPa. A grain boundary can be observed vertically in the middle of the image. The grain on the right of the boundary is ferrite phase, and on the left is martensite phase. Numerous precipitates smaller than 500 nm were formed homogeneously within the ferrite grain. Also, many dislocations, which appeared to be formed during martensitic transformation, are observed within the martensite grain. However, microstructural recovery progressed in parts of the martensite phase, and areas without precipitates and dislocations were also observed.

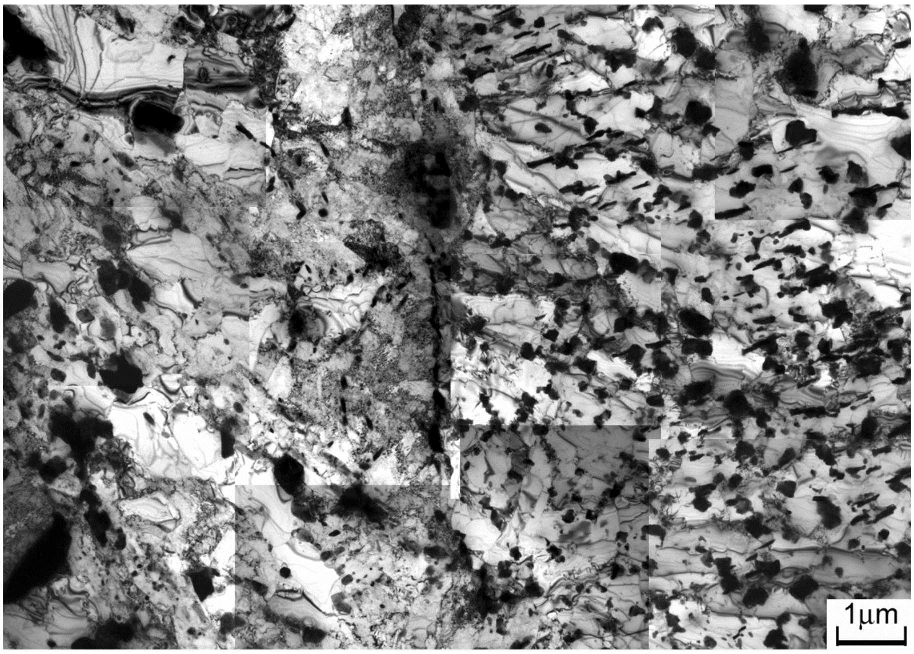

Fig. 8. TEM image of the 0.4%Ni steel creep-ruptured at 923K and 200MPa for 9203.6h.

HOME

The creep strength of the furnace-cooled steels and the nickel-added steels, the volume fraction of the martensite phase in which was relatively large, was inferior, and the recovery of the martensitic microstructure was observed in the creep-ruptured steels. Therefore, martensitic recovery appears to be a cause of the decrease in creep strength of the precipitation-strengthened 15Cr ferritic steels.

4. DISCUSSION

The results of the creep tests and microstructural observations in the present study show that the creep strength of the precipitation-strengthened 15Cr ferritic steel was closely related to the martensite phase and precipitates, i.e., creep strength was weakened with increased volume fraction of the martensite phase and coarse block-type precipitates.

It is generally believed that intermetallic compounds such as the Laves phase are ineffective in improving creep strength in conventional ferritic heat-resistant steels using tempered martensite because of the large coarsening rate of the Laves phase [15, 16]. However, in the 15Cr ferritic steel based on ferrite matrix, the coarsening of intermetallic compounds is slower than that in conventional steels, and their thermal stability is high [9], as is clear from Fig. 6. The precipitation-strengthening effect of fine precipitates and their thermal stability in the ferrite matrix are assumed to be effective in the extension of the creep rupture lives. However, the sparse distribution of coarse block-type particles in the martensite phase reduces the precipitation strengthening effect. Therefore, the solution treatment and water quenching were particularly effective in improving the creep strength, since the faster cooling rate than furnace cooling suppresses the formation of coarse block-type precipitates and the martensite phase. However, the addition of nickel, which is effective in improving the impact toughness of the 15Cr ferritic steel [10, 11], had no effect of extending the creep rupture life, since nickel is an austenite former element, and nickel addition increases the volume fraction of the martensite phase and reduces the precipitation strengthening effect.

Uchida and Fujiwara investigated the effect of nickel content on creep strength and microstructure of a 9Cr-7Mo steel which was developed for use as a core material in advanced fast breeder reactors [17]. This steel is similar to 15Cr ferritic steel in that it depends on precipitation strengthening of intermetallic compounds, solution treatment, and water quenching, although the chromium content is different. Uchida et al. obtained the same results as the present study, i.e., addition of nickel (≈ 3 mass%) reduced the long-term creep strength. Although the fine particles of the Laves phase were precipitated homogeneously within the ferrite grains, the recovery of the martensite phase progressed in addition to minimal precipitates being formed in the martensite phase. Uchida et al. hypothesized that the difference in microstructure between the ferrite and the martensite phase was due to the distribution of several elements; this was confirmed experimentally in the present study.

Several other investigations have been carried out on the effects of nickel addition on the creep strength of conventional ferritic heat-resistant steels with a tempered martensite microstructure [15, 18, 19]. These studies revealed that the addition of nickel decreases the high-temperature creep strength by lowering the A_{c1} transformation temperature and accelerating the recovery of the martensitic matrix.

Almost all these previous studies noted the detrimental effect of nickel on long-term creep strength, as has the present study. However, the addition of more nickel than 1 mass% was required to maintain the high impact toughness of the 15Cr ferritic steel [10, 11]. Therefore, to apply the precipitation-strengthened 15Cr ferritic steel to practical use, it is necessary for the formation of the martensite phase to be suppressed in the solution-treated steels with the addition of nickel by optimization of the chemical composition and heat treatment conditions, such as by reduction of other austenite former elements from the chemical composition or solution treatment at higher temperatures.

HOME

5. CONCLUSIONS

The effects of nickel content and heat treatment conditions on the creep strength of the precipitation-strengthened 15Cr ferritic steel were investigated and the following conclusions obtained.

(1) The creep strength of the 15Cr ferritic steel was drastically improved by the solution treatment and water quenching. The creep strength at 10^4 h of 0.4%Ni steel was doubled, and the creep rupture life at 200 MPa was extended by a factor of about 1000 over the conventional version. However, for the water-quenched steels, over the long term, the detrimental effect of nickel on the creep strength was pronounced.

(2) Although coarse block-type precipitates were observed in the furnace-cooled steels, they were not clearly detectable in the water-quenched steels. The volume fraction of the martensite phase increased with increased nickel content in both the furnace-cooled and water-quenched steels. The volume fraction of the martensite phase in the water-quenched steel was smaller than that in the furnace-cooled version, even at the same nickel content.

(3) Fine particles smaller than 500 nm were precipitated homogeneously within the ferrite phase of the water-quenched steel. On the other hand, coarse block-like particles 1 μm in size were precipitated sparsely within the martensite phase. Recovery of the martensitic microstructure was accelerated.

(4) The martensitic recovery appears to be a cause of decrease in creep strength of precipitation-strengthened 15Cr ferritic steel. Therefore, to enable this steel to be put to practical use, it will be necessary to suppress the formation of the martensite phase caused by addition of Ni by optimizing the chemical composition and heat treatment conditions.

ACKNOWLEDGMENTS

This work was supported by Industrial Technology Research Grant Program in 2003 from the New Energy and Industrial Technology Development Organization (NEDO) of Japan.

REFERENCES

1) F. Masuyama, ISIJ Int., 41, (2001), p.612.
2) T. Matsuo, K. Kimura, R. Tanaka and M. Kikuchi, Proc. of the 4th Int. Conf. on Creep and Fracture of Engineering Materials and Structures, Institute of Materials, London, (1990), p.477.
3) K. Kimura, H. Kushima and F. Abe, Key Eng. Mater., 171-174, (2000), p.483.
4) K. Kimura, H. Kushima, F. Abe, K. Suzuki, S. Kumai and A. Satoh, Proc. of the 7th Int. Conf. on Creep and Fatigue at Elevated Temperatures, JSME, Tokyo, (2001), p.335.
5) K. Kimura, K. Seki, Y. Toda and F. Abe, ISIJ Int., 41, (2001), p.S121.
6) K. Kimura, K. Seki, Y. Toda and F. Abe, J. of Advanced Sci., 13, (2001), p.294.
7) Y. Toda, K. Seki, K. Kimura and F. Abe, JSME Int. J., A45, (2002), p.25.
8) Y. Toda, K. Seki, K. Kimura and F. Abe, ISIJ Int., 43, (2003), p.112.
9) Y. Toda, H. Tohyama, H. Kushima, K. Kimura and F. Abe, JSME Int. J., A48, (2005), p.35.
10) Y. Toda, H. Kushima, K. Kimura and F. Abe, Trans. Mater. Res. Soc. Jpn., 29, (2004), p.3485.
11) Y. Toda, H. Tohyama, H. Kushima, K. Kimura and F. Abe, JSME Int. J., A48, (2005), accepted.
12) Japanese Industrial Standard, “Test Pieces for Tensile Test for Metallic Materials: JIS Z 2201”, Japanese Standard Association, Tokyo, (1998).
13) Data Package for NF616 Ferritic Steel (9Cr-0.5Mo-1.8W-Nb-V), Second Edition, Nippon Steel Corporation, Tokyo, (1994).

HOME

14) F. C. Frank and J. S. Kasper, Acta Cryst., 11, (1958), p.184.
15) H. Cerjak, P. Hofer and B. Schaffernak, ISIJ Int., 39, (1999), p.874.
16) K. Kimura, H. Kushima, F. Abe, K. Suzuki, S. Kumai and A. Satoh, Proc. of the 5th Int. Charles Parsons Turbine Conf., Institute of Materials, London, (2000), p.590.
17) H. Uchida and M. Fujiwara, Tetsu-to-Hagané, 82, (1996), p.87.
18) T. Fujita, K. Yamashita and H. Miyake, Trans. Iron Steel Inst. Jpn., 20, (1980), p.384.
19) M. Fujiwara and H. Uchida, Report of the 123rd Committee on Heat-Resisting Materials and Alloys, Vol. 27, Japan Society for the Promotion of Science, Tokyo, (1986), p.203.

HOME